

Adsorption and migration of single metal atoms on the calcite (10.4) surface

This content has been downloaded from IOPscience. Please scroll down to see the full text.

2017 J. Phys.: Condens. Matter 29 135001

(<http://iopscience.iop.org/0953-8984/29/13/135001>)

View [the table of contents for this issue](#), or go to the [journal homepage](#) for more

Download details:

IP Address: 130.233.243.235

This content was downloaded on 15/02/2017 at 10:59

Please note that [terms and conditions apply](#).

Adsorption and migration of single metal atoms on the calcite (10.4) surface

H Pinto¹, V Haapasilta¹, M Lokhandwala^{1,2}, S Öberg³ and Adam S Foster^{1,4}

¹ COMP, Department of Applied Physics, Aalto University, PO Box 11100, FI-00076 Aalto, Finland

² Department of Electrical Engineering, Indian Institute of Technology Bombay, Mumbai, India

³ Luleå University of Technology, Luleå, Sweden

⁴ Division of Electrical Engineering and Computer Science, Kanazawa University, Kanazawa 920-1192, Japan

E-mail: adam.foster@aalto.fi

Received 14 October 2016, revised 13 January 2017

Accepted for publication 24 January 2017

Published 15 February 2017



Abstract

Transition metal atoms are one of the key ingredients in the formation of functional 2D metal organic coordination networks. Additionally, the co-deposition of metal atoms can play an important role in anchoring the molecular structures to the surface at room temperature. To gain control of such processes requires the understanding of adsorption and diffusion properties of the different transition metals on the target surface. Here, we used density functional theory to investigate the adsorption of 3d (Ti, Cr, Fe, Ni, Cu), 4d (Zr, Nb, Mo, Pd, Ag) and 5d (Hf, W, Ir, Pt, Au) transition metal adatoms on the insulating calcite (10.4) surface. We identified the most stable adsorption sites and calculated binding energies and corresponding ground state structures. We find that the preferential adsorption sites are the Ca–Ca bridge sites. Apart from the Cr, Mo, Cu, Ag and Au all the studied metals bind strongly to the calcite surface. The calculated migration barriers for the representative Ag and Fe atoms indicates that the metal adatoms are mobile on the calcite surface at room temperature. Bader analysis suggests that there is no significant charge transfer between the metal adatoms and the calcite surface.

Keywords: metal adatoms, insulating surface, surface science

(Some figures may appear in colour only in the online journal)

Introduction

Molecular self-assembly is a promising bottom-up technique for the microelectronics industry in the fabrication of devices at nanometer-scale dimensions [1, 2]. Although considerable progress has already been made in the production of nanostructures with tailor-made properties and functionalities by molecular self-assembly, most of the relevant achievements have been made on metallic substrates [3–5].

Electronic, optical and magnetic applications require an insulating substrate to detach the electronic properties of the device from the substrate, as well as a nanostructure that is stable at room temperature since most of the devices operate under ambient conditions [6]. However, the success of molecular self-assembly on insulating surfaces has been limited by the fact that most surface science experimental

techniques require electrically conducting surfaces, and by weak molecule-surface interactions revealed by the systems studied so far [6]. Recently, these difficulties have been addressed using non-contact atomic force microscopy on calcite (10.4) surface. Calcite (CaCO_3) is a bulk insulator and the (10.4) surface is its natural, electrically neutral cleavage plane, on which significant progress has been made in the investigation of molecular self-assembly [7–16].

One potentially promising route towards building nanodevices is to take advantage of metal-organic coordination networks (MOCN): organised networks created via self-assembly of organic linker molecules and coordinating metal atoms [17–19]. Transition metals as coordinating atoms can play an important role by adding functionalities to the molecular structure [20] as well as anchoring the molecular structures to the surface at room temperature. Very recently, the first steps

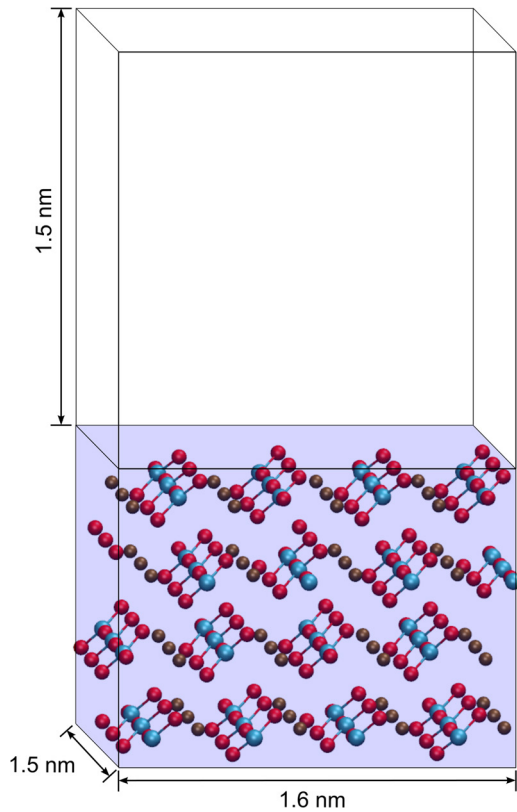


Figure 1. Side view of the calcite (10.4) slab used in the calculations. The slab is made of the repetition of 2×3 unit cells along the $[42.1]$ and $[01.0]$ directions, respectively. In the $[10\bar{1}4]$ direction the slab is composed by four layers of Ca and CO_3 ions separated by a vacuum region of 1.5 nm. The resulting calcite (10.4) surface is charge neutral.

of forming a MOCN on calcite (10.4) surface was achieved by the sequential deposition of biphenyl-4,4-dicarboxylic acid and Fe atoms [21]. Despite the recent progress, the formation of self-assembled structures on insulating surfaces is far from being understood.

Given the relevance that transition metal atoms can play in the development of functional MOCNs, it is crucial to understand their adsorption and diffusion properties. Here we present a study of the adsorption and diffusion properties of $3d$, $4d$ and $5d$ transition metals on calcite (10.4). The binding energies and migration barriers for the different metal atoms on calcite were calculated using density functional theory. Bader charge analysis was used to investigate the charge transfer between the adatoms and the surface.

Methods

The adsorption of metal atoms on the calcite (10.4) surface was studied using density functional theory (DFT) as implemented in the Vienna *Ab Initio* Simulation Package (VASP) code [22, 23]. For the exchange-correlation we use the generalized gradient approximation (GGA) [24, 25] and dispersion corrections were included by using the DFT-D3 method [26, 27]. The atomic cores were replaced by the PAW-type potentials [28, 29] while the valence electrons were represented

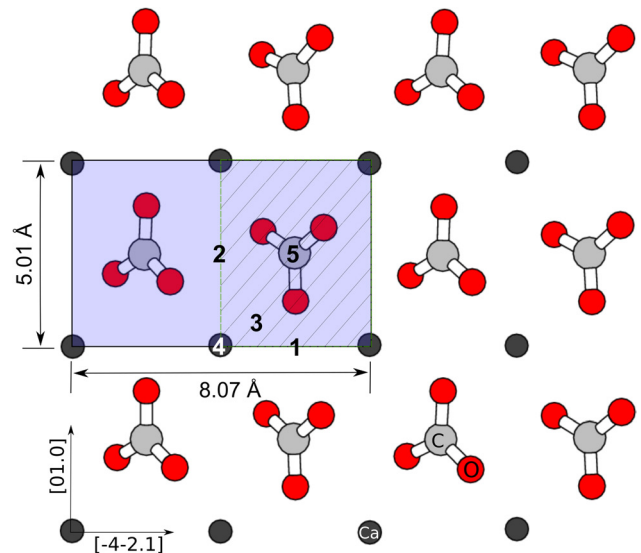


Figure 2. Top view of the calcite (10.4) surface. The C and O atoms are represented in gray and red while the Ca atoms are drawn in black. The dashed blue area shows the unit cell of the surface. The considered binding sites are denoted (1-2) Ca–Ca bridge, (3) Ca–O bridge, (4) Ca top and (5) C top.

by planes waves basis set with a cutoff energy of 450 eV. The Brillouin zone was sampled using a Monkhorst–Pack $2 \times 2 \times 1$ grid ensuring well converged charge density. Since the single adatoms have a magnetic moment, we carried out all calculations spin-polarized.

The calcite (10.4) surface was modelled using a 4 layers slab intercalated by a vacuum region of 1.5 nm to prevent interaction between surfaces, see figure 1. The theoretical lattice parameters calculated for bulk calcite in the hexagonal unit cell, $a = 5.034$ and $c = 16.947$ Å, are within an error smaller than 1% compared to the experimental ones ($a = 4.9896$ and $c = 17.061$ Å [30]).

In this paper we considered $3d$, $4d$, and $5d$ single transition-metal adatoms at five different adsorption sites as shown in figure 2. During the structure optimization the atoms in the bottom two layers of the calcite slab were fixed while all the other atoms were allowed to move until the forces acting on each atom were less than $0.01 \text{ eV } \text{Å}^{-1}$.

The binding energy E_b of the metal atoms on the calcite surface was given by the energy difference between bound and unbound compounds as follows:

$$E_b = E_{\text{total}} - (E_{\text{slab}} + E_{\text{isolated}}) \quad (1)$$

where E_{total} is the energy of the metal adsorbed on the calcite surface, E_{slab} the energy of the bare calcite slab and E_{isolated} the electronic energy of the isolated metal atom.

To investigate the diffusion of metal adatoms across the calcite surface we considered a weakly and strongly bound metal, Ag and Fe respectively. The migration energy barriers were calculated using the nudged elastic band method (NEB) [34, 35] along the most obvious diffusion pathways (see figure 5). The occurrence of charge transfer between the adsorbates and the surface was investigated based on Bader charge analysis [31–33].

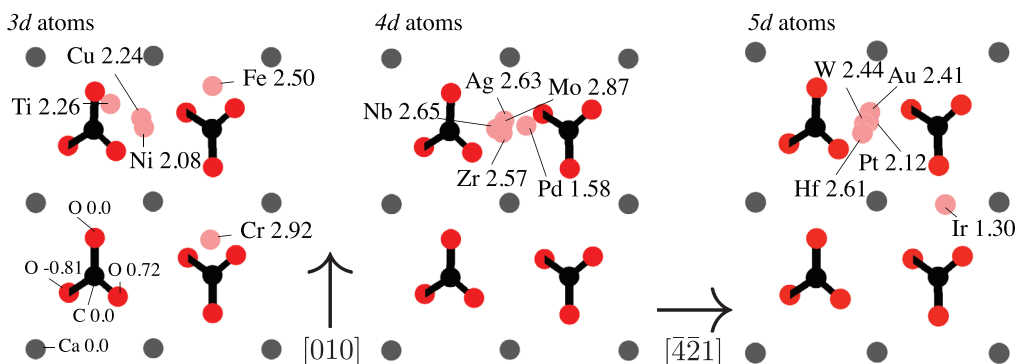


Figure 3. Schematic distribution of the most stable adsorption sites for the metal atoms on calcite (10.4) surface. The C atoms are represented in black, O atoms in red, Ca atoms in grey while all the transition metal atoms are depicted in pink. The adsorption height of each metal atom with respect to the calcite surface plane spanned by carbon and calcium atoms is shown in Ångströms after the element label. It should be noted that the differences in the binding energies between the two Ca–Ca bridge sites are very small. Also, during the optimisation the most reactive metal atoms might cause a notable displacement of the closest surface atoms, not shown in this schematic figure.

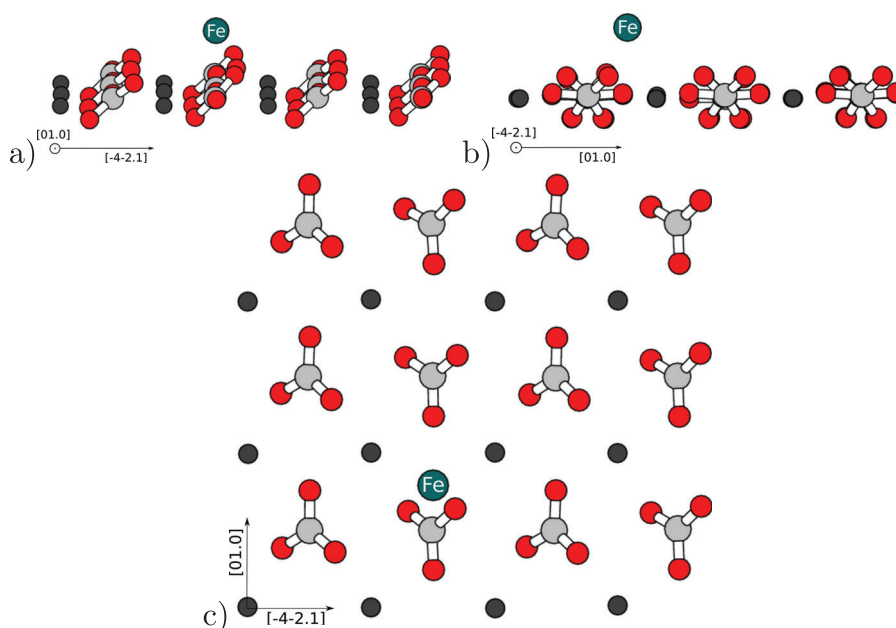


Figure 4. Side (a) [01.0], (b) $[\bar{4}\bar{2}.1]$ and (c) top views of the optimised geometry of the Fe atom on the Ca–Ca $_{[\bar{4}\bar{2}.1]}$ bridge site of the calcite (10.4) surface. After the structure optimisation the Fe atom is displaced from the Ca–Ca $_{[\bar{4}\bar{2}.1]}$ axis towards the nearest protruding oxygen atom.

Results

Firstly, the most stable adsorption sites for the adsorption of the different metal atoms on the calcite (10.4) surface were identified and the binding energies calculated. The distribution of the most stable adsorption sites for the metals on the calcite surface is shown in figure 3. From the five adsorption sites considered here, we found that the Ca–Ca bridge sites, marked 1 and 2 in figure 2, are the preferential adsorption sites for the single adatoms on calcite. In contrast, the Ca–O bridge and Ca top sites, marked 3 and 4 in figure 2, were generally unstable, and during the structure optimisation most of the metal atoms relaxed towards a neighbouring Ca–Ca bridge site. In the case of the C top site, marked 4 in figure 2, some of the studied elements were found to be very reactive with the oxygen atoms of the CO_3^{2-} group. For instance, the adsorption

of Ti, Cr, Fe, Hf and Pt on top of the CO_3^{2-} resulted in the re-orientation of the O atoms or, in the most extreme cases, its detachment from the surface.

As an example, the optimised geometry for the Fe atom in the calcite Ca–Ca $_{[\bar{4}\bar{2}.1]}$ bridge site is shown in figure 4 in more detail. During the structural optimisation the Fe atom moved towards the nearest protruding oxygen. In its fully relaxed configuration the Fe atom sits 1.98 Å away from the oxygen atom and 2.50 Å above the calcite surface plane spanned by the Ca and C atoms.

The calculated binding energies are listed in table 1. The metal adatoms can be categorised according to their binding energies to the calcite surface. We considered the metal adatoms to be weakly bound if the binding energy is larger (more positive) than -1 eV, and strongly bound otherwise. Most of the metals considered here were found to be strongly

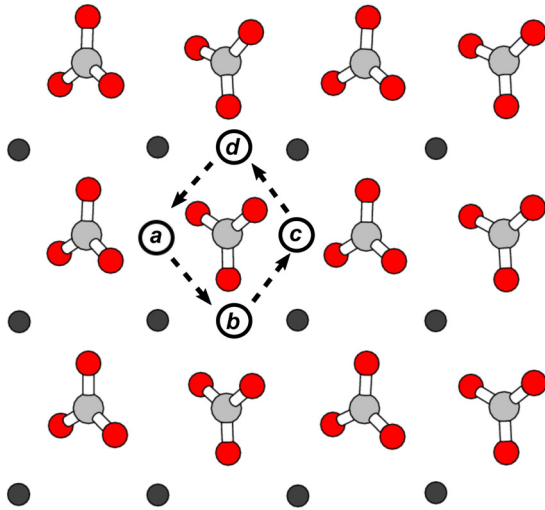


Figure 5. Path for the adatom diffusion via jumps to the nearest Ca–Ca bridge site.

bound, with the exception of Cr, Mo, Cu, Ag and Au. In general, the magnitudes and the trends observed in the adsorption are consistent with earlier computational studies on transition metal adsorption on insulating surfaces, such as on MgO(001) [36] and on MgO(100) [37].

In order to predict the diffusion properties of the metals on the calcite surface which are critical in considering room temperature nanodevice fabrication and operation, we investigated the migration of a weakly and a strongly bound transition metal adatom—Ag and Fe respectively. Here we are assuming that diffusional properties of the adatoms with comparable binding energies are similar. From the binding energies presented above we inferred that the diffusion occurs by hopping between the most favourable adsorption sites as shown in the figure 5. The path across the top of the Ca^{2+} and CO_3^{2-} ions are expected to have a higher barrier. The latter may prevent the diffusion of the metal adatom in the case it strongly reacts with the O atom.

As suggested by the structure optimisation, the surface potential saddle points are located at the bridge sites between the Ca^{2+} and the CO_3^{2-} ions. In the case of Ag the calculated migration barriers are very small, approximately 0.1 eV. For the Fe atom the migration barrier is larger when the atom is hopping between Ca–Ca sites further away from the protruding and in-plane oxygen: 0.56 and 0.60 eV for the a–b and d–a migration paths, respectively (see figure 6). As the Fe atom moves closer to the oxygen atoms the migration barrier drops to 0.31 and 0.11 eV for the b–c and c–d migration paths, respectively.

Using the calculated barriers within transition state theory [38] to obtain estimates for the migration rates r

$$r = \frac{k_B T}{h} \exp\left[-\frac{\Delta E}{k_B T}\right] \quad (2)$$

yields rates from $r = 0.8 \times 10^{12} \text{ s}^{-1}$ to $r = 3 \times 10^3 \text{ s}^{-1}$ for barriers of $\Delta E = 0.1 \text{ eV}$ to $\Delta E = 0.6 \text{ eV}$, respectively, at room temperature ($T = 300 \text{ K}$). In equation (2) k_B and h are the Boltzmann and Planck constants, respectively. We are assuming here that the entropy change in the process is

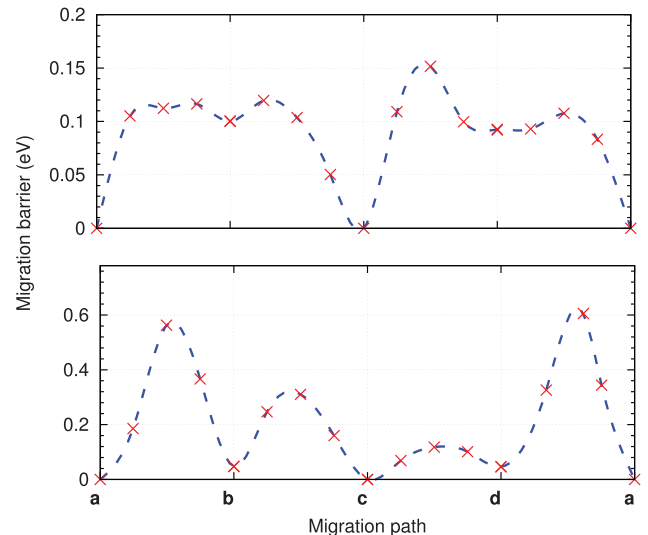


Figure 6. Migration barrier of (top) Ag and (bottom) Fe single atoms hopping to the nearest Ca–Ca bridge site.

Table 1. Calculated binding energy (eV) for the 3d (Ti, Cr, Fe, Ni, Cu), 4d (Zr, Nb, Mo, Pd, Ag) and 5d (Hf, W, Ir, Pt, Au) transition metal adatoms in the most favourable adsorption on (10.4) calcite surface.

	3d				
	Ti	Cr	Fe	Ni	Cu
Ca–Ca _[42.1]	–1.40	–0.63	–1.41	–1.29	–0.64
Ca–Ca _[01.0]	–1.50	–0.58	–1.22	–1.42	–0.75
	4d				
	Zr	Nb	Mo	Pd	Ag
Ca–Ca _[42.1]	–1.24	–1.29	–0.52	–1.14	–0.40
Ca–Ca _[01.0]	–1.27	–1.47	–0.56	–1.58	–0.48
	5d				
	Hf	W	Ir	Pt	Au
Ca–Ca _[42.1]	–1.67	–0.85	–1.40	–1.96	–0.65
Ca–Ca _[01.0]	–1.68	–1.00	–1.32	–1.99	–0.79

negligible, thus these are likely to be lower limits for the actual rates. Nevertheless, these results strongly suggest that the atoms are mobile on the calcite (10.4) surface. Consequently, depending on the concentration of metal atoms on the surface, clustering will take place. In the case of iron such on-surface clustering has been observed experimentally on calcite (10.4) surface, also supported by DFT calculations [21].

A Bader analysis was employed to evaluate the charge transfer between the individual metal adatoms and the calcite surface. Table 2 shows the calculated charge transfer for the different metal atoms in their most stable adsorption configuration on the calcite surface. The direction and magnitude of charge transfer is consistent with the electronegativity trend of the periodic table. Therefore, the least electronegative metals like group-IV Ti, Zr and Hf were found to be the most effective electron donors while the most electronegative group-XI metals Cu, Ag and Au are the most efficient acceptors. It is seen from the table 2 that the largest charge transfer occurs for the Ti atom, with 0.4 e being transferred from the metal to the

Table 2. Charge transfer between the metal atoms and the calcite surface calculated using the Bader analysis. The charge transfer is given by difference between the number of electron of the isolated atom and the atomic charge of the metal adsorbed on calcite surface obtained from Bader. Positive (negative) charge transfer suggests electrons being transferred from (to) the metal to (from) the surface.

3d					
	Ti	Cr	Fe	Ni	Cu
Charge	0.40	0.12	0.06	0.03	0.01
4d					
	Zr	Nb	Mo	Pd	Ag
Charge	0.24	0.14	0.10	0.12	0.03
5d					
	Hf	W	Ir	Pt	Au
Charge	0.18	0.03	-0.11	-0.16	-0.11

calcite surface. In accordance with the small charge transfer, none of the metal atoms induced significant local magnetization upon adsorption.

Conclusions

We studied, from first-principles, the adsorption and diffusion properties of transition metal atoms on the (10.4) calcite surface. The Ca–Ca bridge sites were found to be the most favourable adsorption sites. The top site directly above the Ca^{2+} ion was revealed to be unstable and a strong interaction with the surface oxygen atoms can occur when the metal atoms are placed on top of the CO_3^{2-} group—this may imply restrictions on the choice of metals used, if strong reconstructions of the surface are to be avoided. The calculated binding energies suggest that, apart from the Mo, Cu, Ag and Au, the studied metal atoms bind strongly to the surface. The diffusion properties of the atoms on surface were also studied and the results suggest that most of the considered metals are mobile on the surface at room temperature.

Based on the presented results, it is likely that most metal atoms deposited on the calcite surface will stay adsorbed even at room temperature and diffuse on the surface to the preferred adsorption sites where they will build larger clusters. The knowledge of the most favourable adsorption sites provides important insight for the development of surface templating with calcite. Such information may become especially valuable in designing, creating and analysing metal-molecule co-deposition experiments, suggesting molecule-metal combinations that are more likely to result in successful preparation of assembled networks.

Acknowledgments

This work was supported in part by the Academy of Finland through its Centres of Excellence Programme (2012–2017) under Project No. 251748 and by EU project PAMS (contract no. 610446). We gratefully acknowledge CSC—IT Center for Science Ltd., Espoo for computational resources.

References

- [1] Whitesides G M and Grzybowski B 2002 *Science* **295** 2418
- [2] Barth J V, Costantini G and Kern K 2005 *Nature* **437** 29
- [3] Barth J V 2007 *Annu. Rev. Phys. Chem.* **58** 375
- [4] Kühnle A 2009 *Curr. Opin. Colloid Interface Sci.* **14** 157
- [5] Bartels L 2010 *Nat. Chem.* **2** 87
- [6] Kling F, Bechstein R and Kühnle A 2015 *Non-contact Atomic Force Microscopy (Part of the Series NanoScience and Technology vol 3)* (Berlin: Springer) p 147
- [7] Kittelmann M, Rahe P and Kühnle A 2012 *J. Phys.: Condens. Matter.* **24** 354007
- [8] Kittelmann M, Rahe P, Gourdon A and Kühnle A 2012 *ACS Nano* **6** 7406
- [9] Kittelmann M, Rahe P, Nimmrich M, Hauke C M, Gourdon A and Kühnle A 2011 *ACS Nano* **5** 8420
- [10] Rahe P, Lindner R, Kittelmann M, Nimmrich M and Kühnle A 2012 *Chem. Phys.* **14** 6544
- [11] Rahe P, Nimmrich M and Kühnle A 2012 *Small* **8** 2968
- [12] Hauke C M et al 2013 *ACS Nano* **7** 5491
- [13] Kittelmann M, Nimmrich M, Lindner R, Gourdon A and Kühnle A 2013 *ACS Nano* **7** 5614
- [14] Rahe P, Kittelmann M, Neff J L, Nimmrich M, Reichling M, Maass P and Kühnle A 2013 *Adv. Mater.* **25** 3948
- [15] Kittelmann M, Nimmrich M, Neff J L, Rahe P, Gren W, Bouju X, Gourdon A and Kühnle A 2013 *J. Phys. Chem. C* **117** 23868
- [16] Neff J L, Kittelmann M, Bechstein R and Kühnle A 2014 *Phys. Chem. Chem. Phys.* **16** 15437
- [17] Dong L, Gao Z and Lin N 2016 *Prog. Surf. Sci.* **91** 101
- [18] Barth J V 2009 *Surf. Sci.* **603** 1533
- [19] Stepanow S, Lin N and Barth J V 2008 *J. Phys.: Condens. Matter.* **20** 184002
- [20] Furukawa H, Cordova K E, O’Keeffe M and Yaghi O M 2013 *Science* **341** 974
- [21] Schüller L, Haapasilta V, Kuhn S, Pinto H, Bechstein R, Foster A S and Kühnle A 2016 *J. Phys. Chem. C* **120** 14730
- [22] Kresse G and Furthmüller J 1996 *Phys. Rev. B* **54** 11169
- [23] Paier J et al 2006 *J. Chem. Phys.* **124** 154079
- [24] Perdew J P, Burke K and Ernzerhof M 1996 *Phys. Rev. Lett.* **77** 3865
- [25] Perdew J P, Burke K and Ernzerhof M 1997 *Phys. Rev. Lett.* **78** 1396
- [26] Grimme S, Antony J, Ehrlich S and Krieg S 2010 *J. Chem. Phys.* **132** 154104
- [27] Grimme S, Ehrlich S and Goerigk L 2011 *J. Comput. Chem.* **32** 1456
- [28] Blöchl P E 1994 *Phys. Rev. B* **50** 17953
- [29] Kresse G and Joubert D 1999 *Phys. Rev. B* **59** 1758
- [30] Effenberger H, Mereiter K and Zemann J 1981 *Z. Kristallogr.* **156** 233
- [31] Tang W, Sanville E and Henkelman G 2009 *J. Phys.: Condens. Matter.* **21** 084204
- [32] Sanville E, Kenny S D, Smith R and Henkelman G 2007 *J. Comput. Chem.* **28** 899
- [33] Henkelman G, Arnaldsson A and Jónsson H 2006 *Comput. Mater. Sci.* **36** 254
- [34] Henkelman G and Jónsson H 2000 *J. Chem. Phys.* **113** 9901
- [35] Henkelman G and Jónsson H 2000 *J. Chem. Phys.* **113** 9978
- [36] Neyman K M, Inntam C, Nasluzov V A, Kosarev R and Rösch N 2004 *Appl. Phys. A* **78** 823
- [37] Fernandez S, Markovits A and Minot C 2008 *Chem. Phys. Lett.* **463** 106
- [38] Eyring H 1935 *J. Chem. Phys.* **3** 107